CLIP-170-dependent capture of membrane organelles by microtubules initiates minus-end directed transport

Alexis J. Lomakin[1,2], **Irina Semenova**[1], **Ilya Zaliapin**[3], **Pavel Kraikivski**[1], **Elena Nadezhdina**[4], **Boris M. Slepchenko**[1], **Anna Akhmanova**[5], and **Vladimir Rodionov**[1]

[1]Department of Cell Biology and Center for Cell Analysis and Modeling, University of Connecticut Health Center, Farmington, Connecticut 06032-1507 [2]School of Bionegineering and Bioinformatics, Moscow State Universtiy, Moscow 119992, Russian Federation [3]Department of Mathematics and Statistics, University of Nevada-Reno Reno, NV 89557 [4]Institute of Protein Research, Russian Academy of Sciences, 142290 Pushchino, Moscow Region, Russian Federation [5]Department of Cell Biology, Erasmus Medical Center, 3000 CA Rotterdam, the Netherlands

Summary

Cytoplasmic microtubules (MTs) continuously grow and shorten at free plus ends. During mitosis, this dynamic behavior allows MTs to capture chromosomes to initiate their movement to the spindle poles, however, the role of MT dynamics in capturing organelles for transport in interphase cells has not been demonstrated. Here we used *Xenopus* melanophores to test the hypothesis that MT dynamics significantly contribute to the efficiency of MT minus-end directed transport of membrane organelles. We demonstrated that initiation of transport of membrane-bounded melanosomes (pigment granules) to the cell center involves their capture by MT plus ends, and that inhibition of MT dynamics or loss of the MT plus-end tracking protein CLIP-170 from MT tips dramatically inhibits pigment aggregation. We conclude that MT dynamics are required for the initiation of MT transport of membrane organelles in interphase cells, and that +TIPs such as CLIP-170 play an important role in this process.

Introduction

Cytoplasmic MTs are the major component of the cytoskeleton essential for the spatial organization of cytoplasm (Lane and Allan, 1998; Li and Gundersen, 2008), intracellular transport (Welte, 2004), and cell division (Walczak and Heald, 2008). Minus ends of MTs are often clustered at the MT organizing center, whereas the free plus ends continuously grow and shorten (Mitchison and Kirschner, 1984). This dynamic behavior allows MTs to constantly explore the intracellular space (Kirschner and Mitchison, 1986).

The dynamic behavior of MTs has been shown to play an important role in the initiation of MT-based transport during mitosis. In mitotic cells, the growing ends of MTs capture

kinetochores of chromosomes, and thus enable the movement of chromosomes to the MT minus ends focused at the mitotic spindle poles (Walczak and Heald, 2008). The binding of MT ends to kinetochores involves +TIPs, a group of structurally unrelated proteins highly enriched at the growing MT plus ends (Akhmanova and Steinmetz, 2008; Galjart, 2005; Lansbergen and Akhmanova, 2006; Mimori-Kiyosue and Tsukita, 2003; Morrison, 2007). +TIPs participate in MT-kinetochore interactions, and control the dynamics of the MTs attached to kinetochores (Cheeseman and Desai, 2008; Maiato et al., 2004; Morrison, 2007). It has been proposed that MT dynamics are also important for the interaction of MTs with membrane organelles destined for movement to the MT minus ends in interphase cells, and that p150^{Glued}, which is the large subunit of the dynein activator dynactin and a +TIP, is essential for this process (Vaughan, 2004; Vaughan et al., 2002). However, this hypothesis was questioned by the observation that the loss of p150^{Glued} from MT tips had no detectable effect on membrane trafficking or steady-state distribution of membrane organelles in HeLa cells (Watson and Stephens, 2006). Therefore it remained unclear whether the importance of MT dynamics is specific to mitosis, or plays a more general role in MT transport initiation.

In this study we used *Xenopus* melanophores to test the importance of MT dynamics in initiation of minus-end directed MT transport of membrane organelles in interphase cells. The major function of melanophores is redistribution of thousands of membrane-bounded melanosomes, which aggregate in the cell center or redisperse throughout the cytoplasm (Nascimento et al., 2003). Dispersion involves successive transport of melanosomes to the cell periphery along the radial MTs and randomly arranged actin filaments. For aggregation, melanosomes that move along the actin filaments must transfer onto MTs for transport to the MT minus ends clustered in the cell center (Nascimento et al., 2003). For transfer onto MTs, melanosomes should approach close enough to allow for contact of the melanosome-bound dynein motors with the MT surface. This could occur by means of random movement of melanosomes along the actin filaments, by capturing of melanosomes by the growing MT ends, or both.

Here we examined the mechanism of transfer of melanosomes from actin filaments to MTs during aggregation in more detail. We found that inhibition of actin-based transport in *Xenopus* melanophores did not significantly affect pigment aggregation kinetics, which indicates that it is not important for melanosome transfer from actin filaments to MTs.

Using live cell imaging we observed that the initiation of minus-end transport of melanosomes involved their capture by the growing MT ends. Furthermore, we demonstrated that inhibition of MT growth dramatically suppressed pigment aggregation rate but had no detectable effect on the rate of pigment dispersion. Pigment aggregation was also inhibited by the removal of the +TIP CLIP-170 from MT plus ends, or microinjection of a CLIP-170 antibody. We conclude that MT dynamics are required for the initiation of melanosome transport and that CLIP-170 plays a key role in this process. Therefore our study is the first demonstration of the importance of MT dynamics for transport of membrane organelles in interphase cells.

Results and Discussion

Pigment aggregation requires MT dynamics and involves melanosome capture by growing MT plus ends

Pigment aggregation requires transfer of melanosomes from the actin filaments, which support transport in the dispersed state, onto MTs, which serve as tracks for the movement of melanosomes to the cell center during aggregation (Rodionov et al., 1998; Semenova et al., 2008). To determine whether this transfer depends on the delivery of melanosomes to microtubules by means of transport along actin filaments, we overexpressed in *Xenopus* melanophores the dominant-negative myosin V construct (Rogers et al., 1999), which completely inhibits actin-based transport (Rogers et al., 1999; Semenova et al., 2008). Time-

sequences of phase contrast images of melanophores showed that pigment aggregation in control cells and the cells with inhibited actin transport occurred with very similar rates (Supplemental Videos 1-2). Inhibition of actin transport with the actin-stabilizing drug jasplakinolide also did not reduce the rate of pigment aggregation (Semenova et al., 2008). Lack of significant effect on pigment aggregation indicates that actin-based transport is not important for the transfer of melanosomes from actin filaments onto MTs during pigment aggregation.

To determine whether the transfer process involves capture of melanosomes by growing MT ends, we obtained time-sequences of images of fluorescently labeled MTs and melanosomes in cells treated with melatonin to induce pigment aggregation (Fig. 1A). We found that MTs that grew from the cell center to the periphery frequently contacted melanosomes, and that melanosomes that encountered MTs immediately began moving along them (Fig. 1B, and Supplemental Videos 3-4). Most of the productive binding events ($84.9 \pm 8.5\%$, mean $\pm$ S.D, n= 66), which resulted in transport initiation, occurred at a short distance (3 μm or less) from the MT tip. We conclude that during pigment aggregation, melanosomes are often captured by the growing MT ends.

Next, we examined the effect of MT stabilization on the pigment aggregation rate. We treated melanophores with the drug taxol, known to markedly reduce MT growth and shortening rates (Yvon et al., 1999). Control experiments showed that a brief (10 min) treatment of cells with taxol (1 μM) had no significant effect on cytoplasmic levels of MT polymer or the radial distribution of MTs (data not shown). However, measurement of MT dynamic instability parameters indicated that, as expected, taxol treatment dramatically reduced MT dynamics by causing a ~3-fold decrease in MT growth and shortening rates, and a ~12-fold decrease in the growth and shortening distances (Table 1). To determine whether these changes in MT dynamics affected the ability of cells to aggregate melanosomes, we stimulated pigment aggregation, and 10 min later quantified the fractions of cells with aggregated, partially aggregated, and dispersed melanosomes. We also compared kinetics of pigment aggregation by measuring the values of grey levels within the cell outlines between the control and taxol-treated cells. We found that taxol treatment dramatically inhibited pigment aggregation as evidenced by a substantial increase in the fraction of cells whose pigment remained completely or partially dispersed (Fig. 1C, left), and a significant reduction in the rate of grey level decrease (Fig. 1D, left panel). In contrast to aggregation, taxol treatment did not affect the kinetics of pigment dispersion induced by melanocyte-stimulating hormone (MSH), or the number of cells with dispersed melanosomes in these conditions (Fig. 1C, right, 1D, right). We conclude that MT dynamics are important for melanosome aggregation.

Depletion of CLIP-170 and p150[Glued], but not p150[Glued] alone, from the MT plus ends inhibits pigment aggregation

Live cell imaging experiments demonstrated that pigment aggregation often involved binding of pigment granules to the growing MT ends, which are known to be enriched in +TIPs (Akhmanova and Steinmetz, 2008; Galjart, 2005; Morrison, 2007). Two +TIPs, CLIP-170 and p150[Glued], have been implicated in dynein-based processes, and therefore could potentially participate in the binding of pigment granules to MTs (Akhmanova and Steinmetz, 2008; Galjart, 2005; Lansbergen and Akhmanova, 2006; Morrison, 2007; Schroer, 2004). We therefore examined aggregation of melanosomes in cells lacking CLIP-170 and p150[Glued] at the MT plus ends.

To generate such cells, we took advantage of the known hierarchy of interactions of these proteins with MT tips (Fig. 2A). Targeting of CLIP-170 and p150[Glued] to MT plus ends involves their Cytoskeleton-Associated Protein-Glycine-rich (CAP-Gly) domains. The CAP-Gly domains of CLIP-170 and p150[Glued] bind the C-terminal EEY/F motifs found in several

proteins, which form the MT wall (α-tubulin) or are bound to it (EB proteins EB1 and EB3, and CLIP-170 itself) (Hayashi et al., 2007;Honnappa et al., 2006;Mishima et al., 2007;Weisbrich et al., 2007). Because of the presence of the EEY motif at the α-tubulin C-termini, both CLIP-170 and p150^{Glued} have an intrinsic MT-binding activity (Rickard and Kreis, 1990;Waterman-Storer et al., 1995). However, recent *in vitro* reconstitution conclusively demonstrated that CLIP-170 accumulates at MT tips by a mechanism that requires EB1 (Bieling et al., 2008;Dixit et al., 2009), and involves composite binding sites containing the EEY/F tails of both EB1 and α-tubulin (Bieling et al., 2008). In turn, p150^{Glued} depends on both EB1 and CLIP-170 for plus end accumulation (Lansbergen et al., 2004). MT plus end binding of many other +TIPs is also mediated by EB1, but it is fundamentally different from that of CLIP-170 and p150^{Glued} because it does not depend on the EEY/F tails; instead, it involves interactions of basic-serine rich motifs in +TIPs with EB homology domains of EB proteins (Honnappa et al., 2005;Honnappa et al., 2006;Slep et al., 2005). A unique MT binding mechanism of CLIP-170 and p150^{Glued} allowed us to manipulate the abundance of these proteins at MT plus ends via the overexpression of dominant-negative constructs that inhibited the CAP-Gly- EEY/F interactions.

To remove both CLIP-170 and p150^{Glued} from the MT plus ends, we overexpressed in melanophores the EB family member EB3 that had a GFP tag fused to the C-terminus. We reasoned that an excess of EB3 should displace the endogenous EB1 from the plus ends, and that a large GFP tag attached to the EEY sequence should prevent the recognition of this motif by the endogenous CLIP-170, and inhibit its plus-end targeting (Komarova et al., 2005). CLIP-170-dependent targeting of p150^{Glued} to MT ends would also be inhibited in these conditions. We also used an alternative experimental strategy, which was based on the known ability of the CLIP-170 C-terminus (tail) to bind the N-terminus (head) of CLIP-170 (Lansbergen et al., 2004). Overexpression of the CLIP-170 tail removes the endogenous CLIP-170 from the MT tips because of the blocking of its N-terminal EB1 binding site containing the CAP-Gly domains (Komarova et al., 2002). Since CLIP-170 tail also blocks the MT targeting of CAP-Gly domains of p150^{Glued}, dynactin is also removed from the MT plus ends in the CLIP-170 tail-overexpressing cells, while the levels of plus-end bound EB1 are expected to remain unaffected (Komarova et al., 2002).

In agreement with our expectations, in control non-transfected or GFP-transfected melanophores, EB1, CLIP-170, and p150^{Glued} accumulated at the plus ends of cytoplasmic MTs (Supplemental Figure 1). In marked contrast to control cells, in the EB3-GFP-overexpressing melanophores EB1, CLIP-170, and p150^{Glued} fluorescence was undetectable at the plus ends of a vast majority of MTs (Fig. 2, B and C). We also found that in the GFP-CLIP-170 tail-overexpressing melanophores the endogenous CLIP-170 and p150^{Glued} were missing from MT plus ends, but the levels of endogenous plus-end bound EB1 were not affected (Fig. 2, G and H). We conclude that in agreement with our expectations, overexpression of EB3-GFP and GFP-CLIP-170 tail displaced the endogenous CLIP-170 and p150^{Glued} from MT plus ends (Fig. 2, D and I).

Next, we investigated whether the lack of endogenous CLIP-170 and p150^{Glued} at MT plus ends affected pigment aggregation. We found that the fractions of cells that completely or partially failed to respond to aggregation signals were significantly higher among the EB3-GFP- or GFP-CLIP-170 tail-expressing cells than control GFP-expressing melanophores (Fig. 2, E and J). The pigment aggregation kinetics were also markedly slowed down in the EB3-GFP- or GFP-CLIP-170 tail-expressing cells (Fig. 2, F and K). In contrast to aggregation, dispersion of pigment granules was not affected by the overexpression of EB3-GFP or GFP-CLIP-170 tail (Fig. 2, E and J). Therefore displacement of both CLIP-170 and p150^{Glued} from MT plus ends correlated with a substantial inhibition of pigment aggregation.

To determine the relative importance of CLIP-170 and p150^{Glued} in pigment aggregation, we next examined the behavior of pigment granules in melanophores that specifically lacked the plus-end bound p150^{Glued}. To achieve this, we overexpressed dominant-negative constructs expected to compete with p150^{Glued} for binding to the CLIP-170 C-terminal EEY/F motif - the N-terminal (head) fragment of CLIP-170 and a CLIP-170-binding protein LIS1. We anticipated that an excess of CLIP-170 head should displace p150^{Glued} from the plus ends because of the competition for the C-terminal binding site in the full-length molecule (Hayashi et al., 2007; Lansbergen et al., 2004). The levels of endogenous CLIP-170 should not be affected by CLIP-170 head overexpression, because CLIP-170 head is a monomer, and therefore has lower binding affinity for MT tips than the full-length CLIP-170 dimer. Further, we anticipated that LIS1 would remove p150^{Glued} from MTs because this protein has been shown to interact with the CLIP-170 C-terminus and compete with p150^{Glued} for CLIP-170 binding (Lansbergen et al., 2004; Ligon et al., 2006).

As expected, we found that p150^{Glued} was absent from MT plus ends in the majority of CLIP-170 head- (Fig. 3, A and B) or LIS1- (Fig. 3, F and G) overexpressing cells. In contrast, CLIP-170 and EB1 remained bound to the MT plus ends (Fig. 3, A and B, F and G). Therefore, in the presence of high cytoplasmic levels of CLIP-170 head or LIS1, p150^{Glued} was selectively removed from the plus ends of MTs (Fig. 3, C and H).

We next performed quantitative assays of pigment transport to determine whether the absence of p150^{Glued} from MT plus ends affected pigment aggregation. Remarkably, we found that in cells overexpressing CLIP-170 head or LIS1, aggregation of pigment granules was indistinguishable from control non-transfected or GFP-overexpressing cells (Fig. 3, D and E, I and J). Pigment dispersion was also not affected (Fig 3, D and I). The results of these experiments demonstrated that MT plus-end accumulation of p150^{Glued} is not required for aggregation of pigment granules. We conclude that fast aggregation of pigment granules requires the presence of CLIP-170 but not p150^{Glued} at the MT plus ends.

Binding of melanosomes to MT tips enriched in the GFP-CLIP-170 initiates minus-end directed transport

Our data indicated that the loss of CLIP-170 from MT tips correlated with the inhibition of centripetal transport of melanosomes, and that initiation of melanosome transport occurred predominantly after binding to the ~3 μm-long distal segments of MTs. Therefore, our results suggested that ~3 μm MT segments decorated with CLIP-170 play a significant role in melanosome capture and transport initiation. To further test this hypothesis, we measured the length of comets of endogenous CLIP-170 revealed by immunostaining with a CLIP-170 antibody and found that it was 2.9±0.4 μm (mean±SD) (Supplemental Figure 1), which was very similar to the length of MT segments with enhanced melanosome-binding ability.

Next, we asked whether binding of melanosomes to MT tips decorated with the GFP-CLIP-170 directly leads to initiation of MT transport by performing live cell imaging of GFP-CLIP-170-expressing melanophores treated with melatonin to induce pigment aggregation. As a control we used melanophores expressing EB3-GFP, which displaced CLIP-170 from MT tips (Fig. 2B, C). We observed that during pigment aggregation, GFP-CLIP-170 comets made frequent contacts with melanosomes, and this often led to melanosome movement along MTs (Supplemental Videos 5-7). On average, 74.9±15.7% (mean±SD) of contacts between melanosomes and GFP-CLIP-170-decorated MT ends resulted in MT transport initiation. In contrast, in cells expressing elevated levels of EB3-GFP, the contacts of the vast majority of growing MT tips (93.2±6.8%; mean±SD) with melanosomes did not initiate MT transport (Supplemental Videos 8-10). Therefore, the results of live imaging experiments are consistent with the hypothesis that MT tip-bound CLIP-170 is important in the initiation of MT-based melanosome transport during pigment aggregation.

To further test this hypothesis, we tried a function-blocking approach and examined aggregation of melanosomes in the cells microinjected with a CLIP-170 antibody. Control immunoblotting experiments indicated that in extracts of melanophores the antibody recognized a single polypeptide with a molecular mass of ~170 kDa, similar to CLIP-170 (data not shown). Quantification of the response to pigment-aggregating hormone melatonin indicated that in the population of cells microinjected with the CLIP-170 antibody the fractions of cells with completely and partially dispersed pigment were significantly higher than among the cells injected with non-immune IgG (Supplemenal Figure 2). This result indicates that CLIP-170 antibody significantly inhibited the ability of melanophores to aggregate melanosomes. In contrast, pigment dispersion was not affected by CLIP-170 antibody microinjection (Supplemental Figure 2). Taken together, the results of our experiments indicate that CLIP-170 is required for aggregation of melanosomes and suggest that this protein is directly involved in capture of melanosomes by MTs.

Pigment aggregation defect in cells lacking CLIP-170 at MT tips can be explained by decreased probability of melanosome binding to MT plus ends

Our data pointed to an important role of CLIP-170 in pigment aggregation, and suggested that this molecule could be directly involved in melanosome capture by dynamic MTs. However, other effects of CLIP-170 removal from MT tips on pigment transport were also possible. In mammalian cells, depletion of CLIP-170 from MT tips has been shown to significantly decrease the MT rescue frequency (Komarova et al., 2002). If the same change in MT dynamics occurred in melanophores it could in some way reduce the ability of MTs to bind melanosomes, and therefore inhibit pigment aggregation. It was also possible that the dominant-negative constructs, EB3-GFP and GFP-CLIP-170 tail, which inhibited pigment aggregation, inhibited the minus-end dependent motility of melanosomes independent of the removal of CLIP-170 from MT tips. To investigate these possibilities, we measured parameters of MT dynamic instability and bidirectional MT-based movement of single pigment granules in cells overexpressing dominant-negative constructs that affected the binding of +TIPs to MT plus ends.

We found that overexpression of EB3-GFP, Lis1, and CLIP-170 head or tail domains caused changes in parameters of MT dynamic instability (Table 1). In cells overexpressing CLIP-170 head or tail domains the lengths of MT growth and shortening events increased ~2-fold (Table 1). The CLIP-170 tail overexpression also significantly reduced catastrophe and rescue frequencies (Table 1). We also found that overexpression of dominant-negative constructs affected the parameters of bi-directional movement of single melanosomes. While in most cases changes in these parameters were minor (Table 2), overexpression of CLIP-170 tail caused a substantial (~ 40%) decrease in the average length of minus-end runs of melanosomes. Therefore, overexpression of the dominant-negative +TIP constructs altered MT dynamics and centripetal movement of individual melanosomes along the MTs.

To estimate how changes in the MT dynamics and melanosome movement parameters alter the global pigment density kinetics during aggregation, we developed a 2D stochastic computational model for pigment transport. The model assumed that each melanophore (R=20 μm) contained, on average, 770 melanosomes, and 370 MTs organized into a radial array (Supplemental Table 1; all measurements represent averages for 10 cells). Radial MTs switched between the three states, growth (to the cell periphery), shortening (to the cell center), or pause with frequencies determined by the parameters of MT dynamic instability (Table 1). In the growth state, MTs contacted melanosomes moving along the actin filaments (approximated by diffusion; $D=4\times10^{-3}$ $\mu m^2/s$ (Semenova et al., 2008)) located at a distance ≤0.5 μm (1/2 of the melanosome radius). These contacts initiated movement of melanosomes to the MT minus ends (to the cell center), with the probability 78%. The net velocity of

movement was defined by the parameters of bi-directional MT transport (Table 2). Based on these assumptions and experimentally measured parameters of MT dynamics (Table 1), and MT-based movement of single melanosomes (Table 2), the model computed pigment density kinetics during aggregation.

To test the model, we simulated pigment redistribution in control cells or in cells with taxol-stabilized MTs, and compared the results of simulations with the data obtained in experiments (shown in Figs. 1D, and 2F). This comparison demonstrated a close match between the computed and experimentally measured kinetics (Fig. 4A, and Supplemental Videos 11 and 12), which indicated that fundamental assumptions of the computational model were correct. We next incorporated in the computer simulations parameters of MT dynamics and bi-directional melanosome movement measured in cells overexpressing dominant-negative constructs used in our study (Tables 1 and 2), including GFP-CLIP-170 tail and EB3-GFP, which markedly inhibited pigment aggregation. The results of this analysis showed that the computed pigment aggregation kinetics were in general very similar to the kinetics seen in control GFP-overexpressing cells (Fig. 4B). The predicted kinetics for the GFP-CLIP-170 tail-overexpressing cells (Fig. 4B, red diamonds) were slightly slower compared to control (Fig. 4B, black squares), but still much faster than the experimentally determined kinetics (Fig. 2K). Therefore, changes in the parameters of the MT dynamic instability and bi-directional movement of melanosomes could not explain a dramatic inhibition of pigment aggregation seen in the cells overexpressing dominant-negative +TIP constructs, which displaced CLIP-170 from MT ends (Fig. 2, F and K).

We next used the computational model to examine how the pigment density kinetics during aggregation are affected by a decrease in the binding of melanosomes to MT tips. We found that a 10-fold decrease in the binding probability, which we found in cells overexpressing EB3-GFP, closely reproduced the slow pigment density kinetics seen in these cells (Fig. 4C, and Supplemental Video 13). Therefore computational analysis indicated that reduced kinetics of pigment aggregation seen in cells lacking CLIP-170 at MT plus ends could be fully explained by a decrease in the probability of binding of melanosomes to MT plus ends. This result confirms our hypothesis that the presence of CLIP-170 at the MT plus ends is important for the capturing of melanosomes.

CLIP-170 co-purifies with melanosomes

Our data suggested that the pool of CLIP-170 at MT plus ends was required for melanosome capture during pigment aggregation. It is therefore possible that CLIP-170 at MT plus ends binds melanosomes, and that this binding facilitates MT-based transport to the cell center. An important prediction of this model is that CLIP-170 should be capable of interacting with melanosomes. To test this idea, we purified melanosomes, and probed preparations with a CLIP-170 antibody. Control experiments indicated that melanosome preparations were not contaminated with cytosol, as evidenced by the absence from the melanosome preparations of a soluble protein, glyceraldehyde-3- phosphate dehydrogenase (GAPDH). In contrast to the soluble marker, CLIP-170 was present in preparations of melanosomes isolated from cells with aggregated or dispersed pigment (Fig. 5A). This result is consistent with the role of CLIP-170 in linking melanosomes to MT ends during pigment aggregation.

Conclusions

In this paper we provide evidence that capture of membrane organelles by dynamic MTs can significantly enhance their minus-end-directed transport. Our work for the first time clearly demonstrates the importance of MT dynamics in the initiation of MT minus-end-directed transport in interphase cells, and uncovers a possible role of CLIP-170 in this process. Two features of our experimental system allowed us to detect the kinetic advantage of organelle

loading on dynamic MT ends during minus end-directed transport. First, melanosome aggregation can be induced by an external stimulus, so that a large number of organelles have to be loaded on MTs and transported to the cell center simultaneously, and their kinetics can be easily observed. Second, *Xenopus* melanophores possess a relatively sparse MT system, so that a significant proportion of melanosomes is not in direct contact with MTs when aggregation is initiated. It can be expected that in conditions where minus-end directed movements are infrequent and asynchronous, and the MT network is very dense (like in HeLa cells), kinetic advantages of organelle loading on growing plus ends would have been more difficult to detect.

Based on the results of our experiments we propose a hypothesis for the loading of melanosomes onto MTs for minus-end directed transport (Fig. 5B). We suggest that CLIP-170 bound to the growing plus ends of MTs interacts with a receptor on the melanosome surface. Alternatively, the melanosome-bound CLIP-170 may interact with growing MT plus ends. In any case, CLIP-170-mediated melanosome-MT interaction brings dynein attached to the surface of melanosome in close proximity (touching distance) to the MT wall, and helps to initiate minus-end directed transport.

Interactions between +TIPs at growing microtubule ends and specific receptors on the membrane surface might control different aspects of membrane dynamics. Support for this model comes from the recent observation that ER membranes can directly bind to MT tip-bound EB1 through a transmembrane ER-resident protein STIM1 (Grigoriev et al., 2008). Different classes of vesicular carriers can be delivered from one compartment to the next along cytoplasmic MTs, and their centripetal movement usually involves cytoplasmic dynein (Caviston and Holzbaur, 2006; Lane and Allan, 1998). We hypothesize that, similar to melanosomes, other membrane-bounded compartments destined for minus-end directed MT transport might be captured by the tips of dynamic MTs. Testing the predictions of this hypothesis is an exciting direction for the future research.

Experimental Procedures

Cell culture and taxol treatment

Xenopus melanophore cell lines (Kashina et al., 2004) were cultured in *Xenopus* tissue culture medium (70% L15 medium supplemented with antibiotics, 20% fetal bovine serum, and 5 μg/ml insulin) at 27°C. To induce pigment aggregation or dispersion, cells were placed in a serum-free medium 1 hr before the hormone addition. Pigment aggregation was induced with 10^{-8} M melatonin. To induce pigment dispersion, cells were washed 3-5 times with a serum-free medium to remove melatonin, and treated with MSH (10^{-8} M). To stabilize cytoplasmic MTs, melanophores were treated with taxol (1 μM) for 10 min.

Fluorescence labeling of MTs and live cell imaging

For fluorescence labeling of MTs, melanophores were pressure microinjected with Cy3-tagged bovine brain tubulin prepared as described previously (Semenova and Rodionov, 2007). Injected cells were incubated for at least one hour at 27°C to allow for the incorporation of labeled tubulin into MTs.

Fluorescence images of cells were acquired using a Nikon Eclipse TE300 inverted microscope equipped with a Plan x100 1.25 NA objective lens. Fluorescence images of Cy3-labeled MTs were obtained with Andor iXon EM-CCD sensor (Andor Technology, Windsor, CT) driven by Metamorph image acquisition and analysis software (Universal Imaging, Downington, PA). To reduce photobleaching and photodamage, cells were treated the oxygen-depleting agent

Oxyrase (Oxyrase Company, Mansfield, OH) prior to image acquisition (Semenova and Rodionov, 2007).

Phase-contrast and brightfield images of melanophores were obtained with Watec-902B charged coupled device camera (Watec Corp., Japan) driven by Metamorph.

The movement of individual melanosomes was recorded and analyzed as described previously (Zaliapin et al., 2005). The data were collected 2.5 min after the stimulation of cells with melatonin.

Quantification of aggregation and dispersion of melanosomes

To determine the fractions of aggregated, partially aggregated, or dispersed cells, melanophores were treated with melatonin or MSH for 10 and 15 min, respectively, and fixed with formaldehyde. The number of cells with aggregated, partially aggregated, or dispersed pigment were determined by counting cells in each category under a phase-contrast microscope, as described previously (Kashina et al., 2004).

To determine kinetics of pigment aggregation or dispersion, time-series of bright-field images of melanophores treated with melatonin or MSH to stimulate pigment aggregation or dispersion, respectively, were acquired with 10 s time intervals. Integrated pixel values within cell outlines were determined for each of the acquired images in a time-series using the Metamorph region measurement tool. The value in the fully dispersed state was taken as 100%. Percentage of grey levels was calculated for each image using the equation:

$$A = I_b - I_f / (I_b - I_d) \times 100$$

where I_b is normalized background levels measured outside the cell outlines, I_t is integrated pixel value within a cell outline at a given moment t, and I_d is integrated pixel value within a cell outline in the fully dispersed state. Percentages of black levels for each time point were averaged across the recorded cells, and plotted as a function of time. Data on each plot represents averaging for at least 20 cells.

DNA constructs and transfection

GFP-CLIP-170 head (amino acids 4-309 of rat brain CLIP-170 cDNA) and tail (amino acids 1,027-1,320) were described by (Komarova et al., 2002); EB3-GFP was described by (Stepanova et al., 2003); GFP-LIS1 was described by (Coquelle et al., 2002). The dominant-negative myosin V construct, GFP-MST (Rogers et al., 1999), was a gift from Dr. Vladimir Gelfand.

Cells were transfected using Lipofectamine 2000 (Invitrogen Corp., Carlsbad, CA) according to the manufacturer's instructions, and incubated for 2-3 days at 27°C to allow for protein expression.

Immunostaining

For immunostaining, cells were briefly rinsed with PBS, fixed in cold methanol (-20°C) and double immunostained with antibodies against a +TIP and tubulin. Primary antibodies were rabbit polyclonal antibodies specific for CLIP-170 C-terminus (no. 2360, 1:200) (Coquelle et al., 2002), and N-terminus of CLIP-170 and CLIP-115 (no. 2221, ref. 1:200) (Hoogenraad et al., 2000), sheep polyclonal antibody specific for tubulin (Cytoskeleton, Inc., Denver, CO, 1:100), mouse monoclonal antibodies against EB1 (1:100) and p150[Glued] (1:200; both from BD Transduction Laboratories, Franklin Lakes, NJ), and rat monoclonal anti-tubulin antibody

(clone CBL270, Millipore Corp., Billerica, MA). Secondary antibodies were Alexa Fluor 488-conjugated goat anti-mouse and goat anti-rabbit IgG (1:100, Invitrogen Corp., Carlsbad, CA), TRITC-conjugated donkey anti-rabbit and anti-mouse IgG (1:100, Jackson ImmunoResearch Laboratories, West Grove, PA), and Cy5-conjugated anti-rat IgG (1:100, Jackson ImmunoResearch Laboratories, West Grove, PA). Stained cells were mounted in Aqua-PolyMount medium (Polysciences Inc., Warrington, PA).

Purification of melanosomes and immunoblotting

Melanosomes were purified as described previously (Kashina et al., 2004). Immunoblotting was performed as described by (Towbin et al., 1979), using a polyclonal CLIP-170 antibody (H300; Santa Cruz Biotechnology, Santa Cruz, CA, or 2360, Coquelle et al., 2002) or antibody against glyceraldehyde-3-phosphate dehydrogenase (clone 6C5, Millipore Corp., Billerica, MA). Immunoreactive bands were detected with SuperSignal West Femto maximum sensitivity substrate (Pierce Biotechnology, Inc., Rockford, IL).

Microinjectin of a CLIP-170 antibody

Rabbit monospecific antibody raised against CLIP-170 (H300; Santa Cruz Biotechnology, Santa Cruz, CA) was pressure-microinjected at needle concentration 12 mg/ml. Rabbit non-immune IgG taken at the same concentration were used for control microinjections. Cells were treated with melatonin (10 min) or MSH (15 min) to induce pigment aggregation or dispersion, respectively, and fixed with 4% paraformaldehyde. Microinjected cells were identified by immunostaining with goat anti-rabbit IgG conjugated with Alexa 488 (Invitrogen Corp., Carlsbad, CA).

Supplementary Material

Refer to Web version on PubMed Central for supplementary material.

Acknowledgments

References

Akhmanova A, Steinmetz MO. Tracking the ends: a dynamic protein network controls the fate of microtubule tips. Nat Rev Mol Cell Biol 2008;9:309–322. [PubMed: 18322465]

Bieling P, Kandels-Lewis S, Telley IA, van Dijk J, Janke C, Surrey T. CLIP-170 tracks growing microtubule ends by dynamically recognizing composite EB1/tubulin-binding sites. J Cell Biol 2008;183:1223–1233. [PubMed: 19103809]

Caviston JP, Holzbaur EL. Microtubule motors at the intersection of trafficking and transport. Trends Cell Biol 2006;16:530–537. [PubMed: 16938456]

Cheeseman IM, Desai A. Molecular architecture of the kinetochoremicrotubule interface. Nat Rev Mol Cell Biol 2008;9:33–46. [PubMed: 18097444]

Coquelle FM, Caspi M, Cordelieres FP, Dompierre JP, Dujardin DL, Koifman C, Martin P, Hoogenraad CC, Akhmanova A, Galjart N, et al. LIS1, CLIP-170's key to the dynein/dynactin pathway. Mol Cell Biol 2002;22:3089–3102. [PubMed: 11940666]

Dixit R, Barnett B, Lazarus JE, Tokito M, Goldman YE, Holzbaur EL. Microtubule plus-end tracking by CLIP-170 requires EB1. Proc Natl Acad Sci U S A 2009;106:492–497. [PubMed: 19126680]

Galjart N. CLIPs and CLASPs and cellular dynamics. Nat Rev Mol Cell Biol 2005;6:487–498. [PubMed: 15928712]

Grigoriev I, Gouveia SM, van der Vaart B, Demmers J, Smyth JT, Honnappa S, Splinter D, Steinmetz MO, Putney JW Jr. Hoogenraad CC, Akhmanova A. STIM1 is a MT-plus-end-tracking protein involved in remodeling of the ER. Curr Biol 2008;18:177–182. [PubMed: 18249114]

Hayashi I, Plevin MJ, Ikura M. CLIP170 autoinhibition mimics intermolecular interactions with p150Glued or EB1. Nat Struct Mol Biol 2007;14:980–981. [PubMed: 17828275]

Honnappa S, John CM, Kostrewa D, Winkler FK, Steinmetz MO. Structural insights into the EB1-APC interaction. Embo J 2005;24:261–269. [PubMed: 15616574]

Honnappa S, Okhrimenko O, Jaussi R, Jawhari H, Jelesarov I, Winkler FK, Steinmetz MO. Key interaction modes of dynamic +TIP networks. Mol Cell 2006;23:663–671. [PubMed: 16949363]

Hoogenraad CC, Akhmanova A, Grosveld F, De Zeeuw CI, Galjart N. Functional analysis of CLIP-115 and its binding to microtubules. J Cell Sci 2000;113(Pt 12):2285–2297. [PubMed: 10825300]

Kashina A, Rodionov V. Actin dynamics is essential for myosin-based transport of membrane organelles. Curr Biol 2008;18:1581–1586. [PubMed: 18951026]

Kashina AS, Semenova IV, Ivanov PA, Potekhina ES, Zaliapin I, Rodionov VI. Protein kinase A, which regulates intracellular transport, forms complexes with molecular motors on organelles. Curr Biol 2004;14:1877–1881. [PubMed: 15498498]

Kirschner M, Mitchison T. Beyond self-assembly: from microtubules to morphogenesis. Cell 1986;45:329–342. [PubMed: 3516413]

Komarova Y, Lansbergen G, Galjart N, Grosveld F, Borisy GG, Akhmanova A. EB1 and EB3 control CLIP dissociation from the ends of growing microtubules. Mol Biol Cell 2005;16:5334–5345. [PubMed: 16148041]

Komarova YA, Akhmanova AS, Kojima S, Galjart N, Borisy GG. Cytoplasmic linker proteins promote microtubule rescue in vivo. J Cell Biol 2002;159:589–599. [PubMed: 12446741]

Lane J, Allan V. Microtubule-based membrane movement. Biochim Biophys Acta 1998;1376:27–55. [PubMed: 9666066]

Lansbergen G, Akhmanova A. Microtubule plus end: a hub of cellular activities. Traffic 2006;7:499–507. [PubMed: 16643273]

Lansbergen G, Komarova Y, Modesti M, Wyman C, Hoogenraad CC, Goodson HV, Lemaitre RP, Drechsel DN, van Munster E, Gadella TW Jr. et al. Conformational changes in CLIP-170 regulate its binding to microtubules and dynactin localization. J Cell Biol 2004;166:1003–1014. [PubMed: 15381688]

Li R, Gundersen GG. Beyond polymer polarity: how the cytoskeleton builds a polarized cell. Nat Rev Mol Cell Biol 2008;9:860–873. [PubMed: 18946475]

Ligon LA, Shelly SS, Tokito MK, Holzbaur EL. Microtubule binding proteins CLIP-170, EB1, and p150Glued form distinct plus-end complexes. FEBS Lett 2006;580:1327–1332. [PubMed: 16455083]

Maiato H, DeLuca J, Salmon ED, Earnshaw WC. The dynamic kinetochore-microtubule interface. J Cell Sci 2004;117:5461–5477. [PubMed: 15509863]

Mimori-Kiyosue Y, Tsukita S. "Search-and-capture" of microtubules through plus-end-binding proteins (+TIPs). J Biochem 2003;134:321–326. [PubMed: 14561716]

Mishima M, Maesaki R, Kasa M, Watanabe T, Fukata M, Kaibuchi K, Hakoshima T. Structural basis for tubulin recognition by cytoplasmic linker protein 170 and its autoinhibition. Proc Natl Acad Sci U S A 2007;104:10346–10351. [PubMed: 17563362]

Mitchison T, Kirschner M. Dynamic instability of microtubule growth. Nature 1984;312:237–242. [PubMed: 6504138]

Morrison EE. Action and interactions at microtubule ends. Cell Mol Life Sci 2007;64:307–317. [PubMed: 17221167]

Nascimento AA, Roland JT, Gelfand VI. Pigment cells: a model for the study of organelle transport. Annu Rev Cell Dev Biol 2003;19:469–491. [PubMed: 14570578]

Rickard JE, Kreis TE. Identification of a novel nucleotide-sensitive microtubule-binding protein in HeLa cells. J Cell Biol 1990;110:1623–1633. [PubMed: 1970824]

Rodionov VI, Hope AJ, Svitkina TM, Borisy GG. Functional coordination of microtubule-based and actin-based motility in melanophores. Curr Biol 1998;8:165–168. [PubMed: 9443917]

Rogers SL, Karcher RL, Roland JT, Minin AA, Steffen W, Gelfand VI. Regulation of melanosome movement in the cell cycle by reversible association with myosin V. J Cell Biol 1999;146:1265–1276. [PubMed: 10491390]

Schroer TA. Dynactin. Annu Rev Cell Dev Biol 2004;20:759–779. [PubMed: 15473859]

Semenova I, Burakov A, Berardone N, Zaliapin I, Slepchenko B, Svitkina T, Semenova I, Rodionov V. Fluorescence microscopy of microtubules in cultured cells. Methods Mol Med 2007;137:93–102. [PubMed: 18085223]

Slep KC, Rogers SL, Elliott SL, Ohkura H, Kolodziej PA, Vale RD. Structural determinants for EB1-mediated recruitment of APC and spectraplakins to the microtubule plus end. J Cell Biol 2005;168:587–598. [PubMed: 15699215]

Stepanova T, Slemmer J, Hoogenraad CC, Lansbergen G, Dortland B, De Zeeuw CI, Grosveld F, van Cappellen G, Akhmanova A, Galjart N. Visualization of microtubule growth in cultured neurons via the use of EB3-GFP (end-binding protein 3-green fluorescent protein). J Neurosci 2003;23:2655–2664. [PubMed: 12684451]

Towbin H, Staehelin T, Gordon J. Electrophoretic transfer of proteins from polyacrylamide gels to nitrocellulose sheets: procedure and some applications. Proc Natl Acad Sci U S A 1979;76:4350–4354. [PubMed: 388439]

Vaughan KT. Surfing, regulating and capturing: are all microtubule-tip-tracking proteins created equal? Trends Cell Biol 2004;14:491–496. [PubMed: 15350977]

Vaughan PS, Miura P, Henderson M, Byrne B, Vaughan KT. A role for regulated binding of p150(Glued) to microtubule plus ends in organelle transport. J Cell Biol 2002;158:305–319. [PubMed: 12119357]

Walczak CE, Heald R. Mechanisms of mitotic spindle assembly and function. Int Rev Cytol 2008;265:111–158. [PubMed: 18275887]

Waterman-Storer CM, Karki S, Holzbaur EL. The p150Glued component of the dynactin complex binds to both microtubules and the actin-related protein centractin (Arp-1). Proc Natl Acad Sci U S A 1995;92:1634–1638. [PubMed: 7878030]

Watson P, Stephens DJ. Microtubule plus-end loading of p150(Glued) is mediated by EB1 and CLIP-170 but is not required for intracellular membrane traffic in mammalian cells. J Cell Sci 2006;119:2758–2767. [PubMed: 16772339]

Weisbrich A, Honnappa S, Jaussi R, Okhrimenko O, Frey D, Jelesarov I, Akhmanova A, Steinmetz MO. Structure-function relationship of CAPGly domains. Nat Struct Mol Biol 2007;14:959–967. [PubMed: 17828277]

Welte MA. Bidirectional transport along microtubules. Curr Biol 2004;14:R525–537. [PubMed: 15242636]

Yvon AM, Wadsworth P, Jordan MA. Taxol suppresses dynamics of individual microtubules in living human tumor cells. Mol Biol Cell 1999;10:947–959. [PubMed: 10198049]

Zaliapin I, Semenova I, Kashina A, Rodionov V. Multiscale trend analysis of microtubule transport in melanophores. Biophys J 2005;88:4008–4016. [PubMed: 15764663]
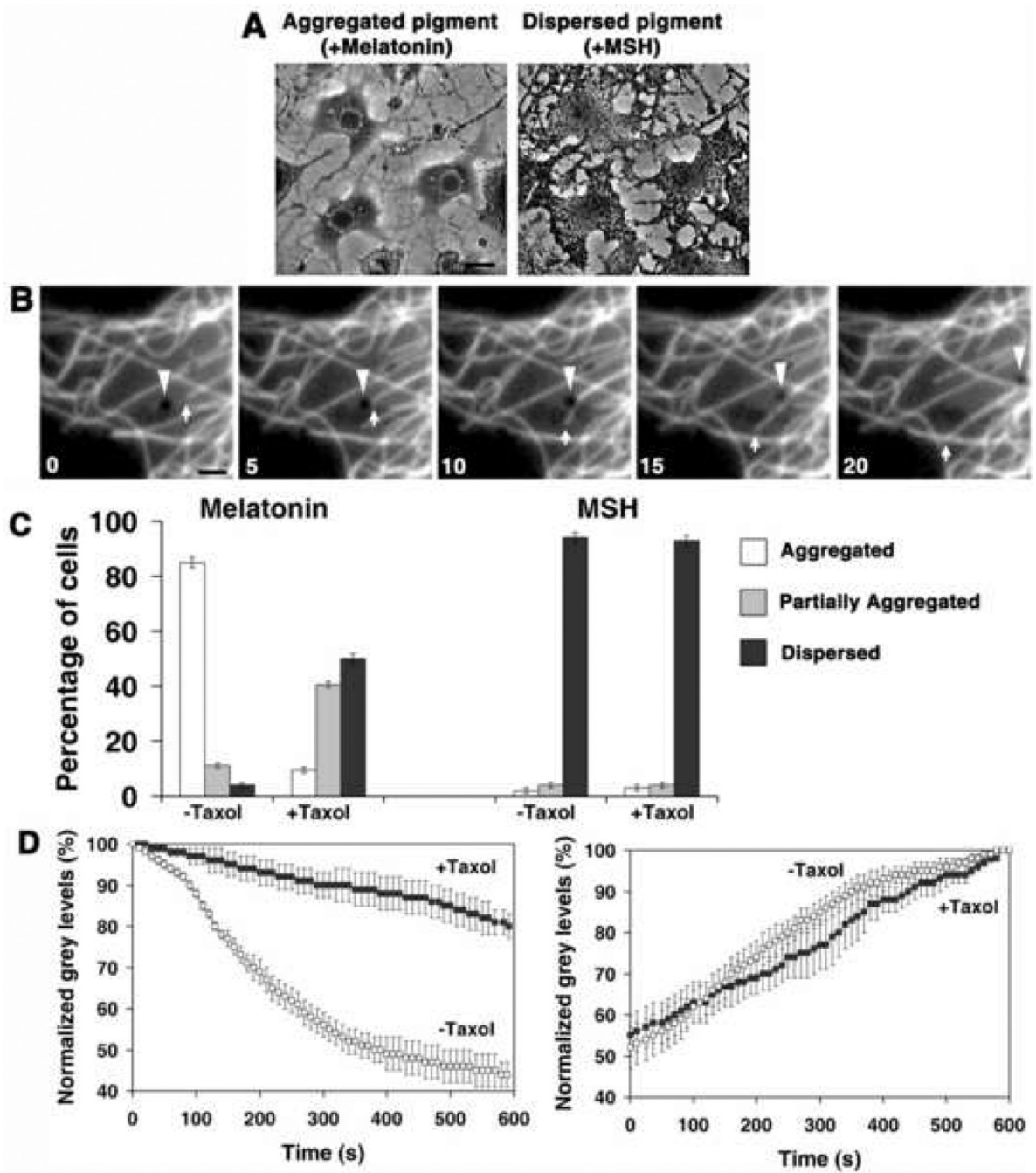
Figure 1. Stabilization of microtubules with taxol inhibits aggregation of melanosomes
(A) Phase-contrast images of melanophores treated with MSH (left) or melatonin (right) to disperse or aggregate melanosomes. Bar, 20 μm. (B) Time series of images of a melanophore with fluorescently labeled MTs treated with melatonin to induce pigment aggregation; after capture by the growing MT tip (arrow) a melanosome (arrowhead) starts moving along the MT toward the cell center. Bar, 2 μm. See also Supplemental Videos 3 and 4. (C) Quantification of responses to melatonin or MSH, applied to induce pigment aggregation or dispersion, of control non-treated melanophores or melanophores treated with the MT-stabilizing drug taxol; the data are expressed as the percentages of cells with aggregated (white bars), partially dispersed (grey bars) or completely dispersed (black bars) pigment. Quantification was

performed at 10 min (aggregation) or 15 min (dispersion) after stimulation.(D) Quantification of kinetics of pigment aggregation (left panel) or dispersion (right panel) in control non-treated (white squares) or taxol-treated (black squares) melanophores; data are expressed as the percentage of change with time in the grey levels within the cell outlines; 100% corresponds to the fully dispersed state.
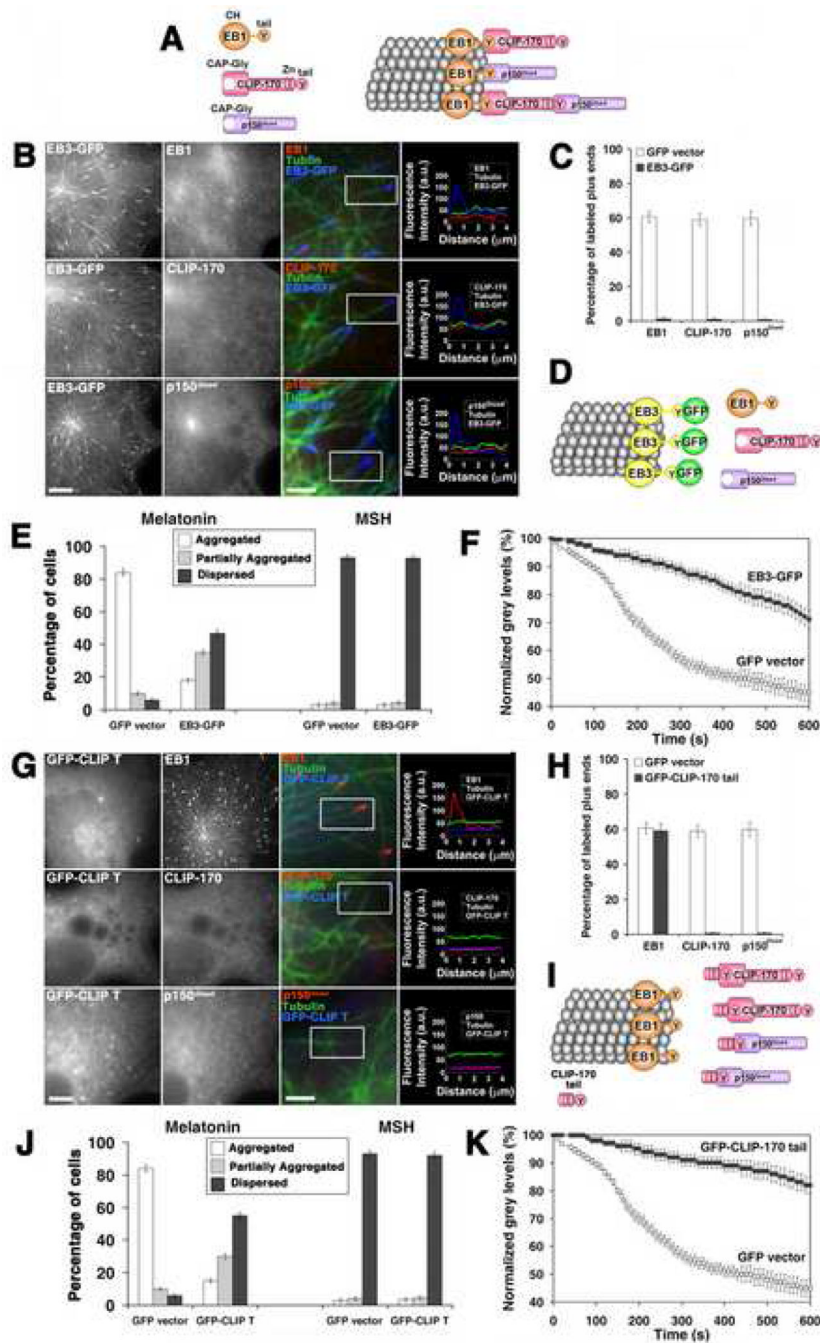
Figure 2. Overexpression of EB3-GFP or GFP-CLIP-170 tail removes CLIP-170 and p150^{Glued} from the plus ends of MTs, and inhibit pigment aggregation

(A) Hierarchy of plus-end accumulation of +TIPs: p150^{Glued} binds MT plus ends via CLIP-170 or EB1, CLIP-170 binding is mediated by EB1, and EB1 directly binds tubulin molecules in the MT wall; CLIP-170 and p150^{Glued} can bind tubulin directly, and these interactions contribute to their plus-end localization, but are not sufficient to mediate it, and therefore are not shown. (B and G) Immunostaining of EB3-GFP-overexpressing (B) or GFP-CLIP-170 tail-overexpressing (G) cells with antibodies against EB1, CLIP-170, or p150^{Glued}; examples of low and high magnification images are shown for each +TIP (with color codes indicated above the merged images). Representative line scan analyses of protein accumulation at MT tips in

the boxed regions are shown on the right. Bars, 10 μm (left columns) or 2.5 μm (middle columns). (C and H) Fractions of MT plus ends immunostained for EB1, CLIP-170, or p150^{Glued} in the EB3-GFP-overexpressing (C) or GFP-CLIP-170 tail-overexpressing (H) cells. (D and I) Diagrams illustrating the effect of EB3-GFP (D) or CLIP-170 tail (I) overexpression on the composition of +TIPs at MT plus ends; EB3-GFP displaces all major +TIPs (EB1, CLIP-170, and p150^{Glued}) from MT plus ends, whereas GFP-CLIP-170 tail displaces CLIP-170, and p150^{Glued}, but not EB1. (E and J) Quantification of responses of EB3-GFP (E) or GFP-CLIP-170 tail-overexpressing (J) cells to melatonin or MSH; the data is expressed as the percentages of cells with aggregated (white bars), partially dispersed (grey bars) or completely dispersed (black bars) pigment. (F and K) Quantification of kinetics of pigment aggregation in the cells overexpressing EB3-GFP (F) or GFP-CLIP-170 (K); the data is expressed as a decrease in the values the grey levels within the cell outlines with time.
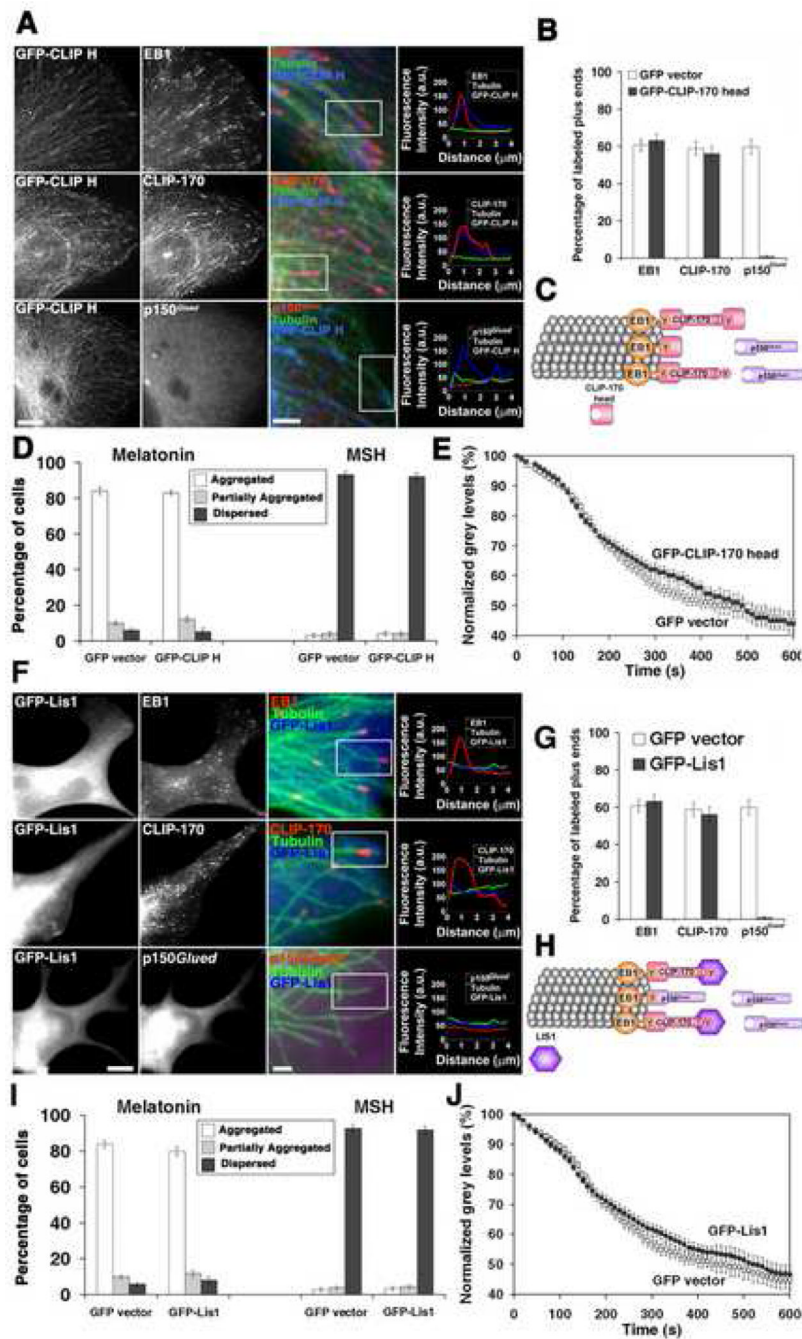
Figure 3. Overexpression of the CLIP-170 head or LIS1 displace p150[Glued] from MT plus ends, but does not affect pigment aggregation

(A and F) Immunostaining of cells overexpressing GFP-CLIP-170 head or GFP-LIS1 with antibodies against EB1, CLIP-170, or p150[Glued]; examples of low and high magnification images are shown for each +TIP (with color codes indicated above the merged images). Representative line scan analyses of protein accumulation at MT tips are shown on the right. Bars, 10 μm (left columns) or 2.5 μm (middle columns). (B and G) Fractions of MT plus ends immunostained for EB1, CLIP-170 or p150[Glued] in the GFP-CLIP-170 head- (B) or GFP-LIS1- (G) overexpressing cells. (C and H) Diagrams illustrating the effects of CLIP-170 head (C) or LIS1 (H) overexpression on the composition of +TIPs at MT plus ends; CLIP-170 head or

LIS1 displace p150^{Glued}, but not CLIP-170 or EB1 from the MT plus ends. (D and I) Quantification of responses of GFP-CLIP-170 head (D) or GFP-LIS1- (I) overexpressing cells to melatonin or MSH; the data is expressed as the percentages of cells with aggregated (white bars), partially dispersed (grey bars) or completely dispersed (black bars) pigment. (E and J) Quantification of kinetics of pigment aggregation in the cells overexpressing GFP-CLIP-170 head (E) or GFP-LIS1 (J); the data is expressed as a decrease in the values the grey levels within the cell outlines with time.
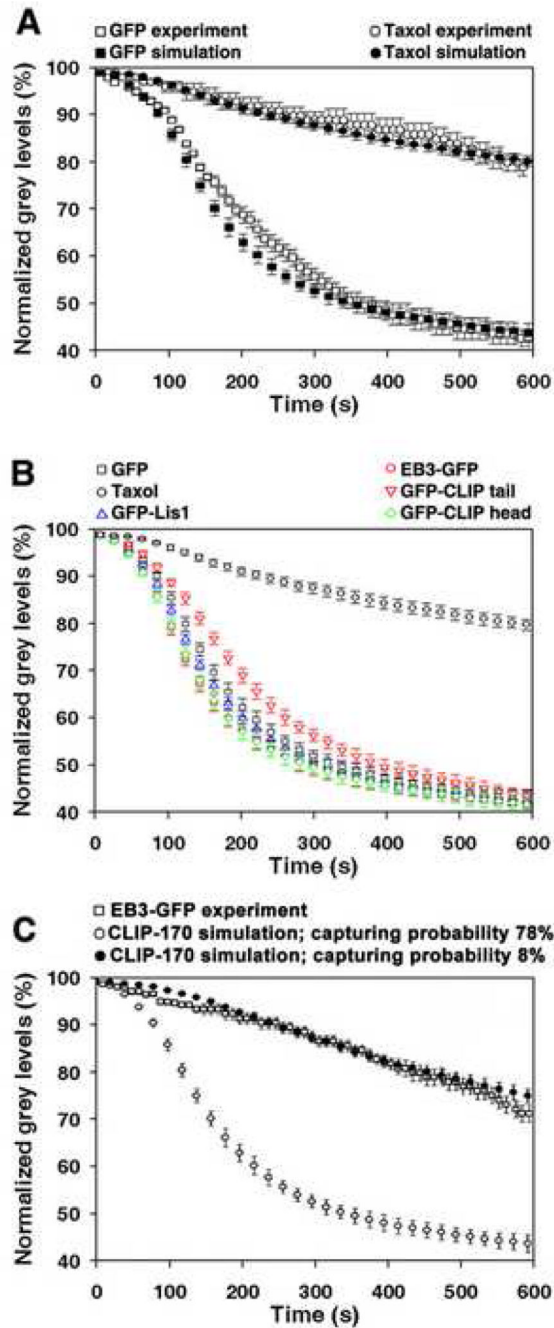
Figure 4. Changes in the parameters of MT dynamic instability and bidirectional movement of melanosomes along MTs do not affect significantly pigment aggregation kinetics
(A) Comparison of kinetics of pigment aggregation for cells overexpressing GFP or treated with taxol determined experimentally (open symbols), or computed using the parameters of MT dynamic instability and bi-directional melanosome movement shown in Tables 1 and 2 (filled symbols). Data are expressed as the percentage of change with time in the grey levels within the cell outlines. Computational simulations accurately reproduce kinetics of pigment aggregation in the presence (circles) or absence (squares) of taxol. (B) Computed kinetics of pigment aggregation for the taxol-treated cells, or cells overexpressing GFP, EB3-GFP, GFP-CLIP-170 tail, GFP-CLIP-170 head, or GFPLIS1. Overexpression of dominant-negative

constructs, which alter the composition of +TIPs at the MT plus ends (EB3-GFP, GFP-CLIP-170 tail, GFP-CLIP-170 head, or GFPLIS1), does not significantly inhibit pigment aggregation kinetics. (C) Comparison of the kinetics of pigment aggregation experimentally measured in the cells overexpressing EB3-GFP (open squares), with the kinetics computed with the assumption that the probability of capturing of melanosomes by the CLIP-170-enriched MT plus ends is 78% (open circles) or 8% (closed circles). The kinetics computed at a low capturing probability closely matches the EB3-GFP kinetics, which confirms that a decreased pigment aggregation rate seen in cells lacking CLIP-170 at the MT plus ends could be explained by a reduced capturing ability of MTs alone.
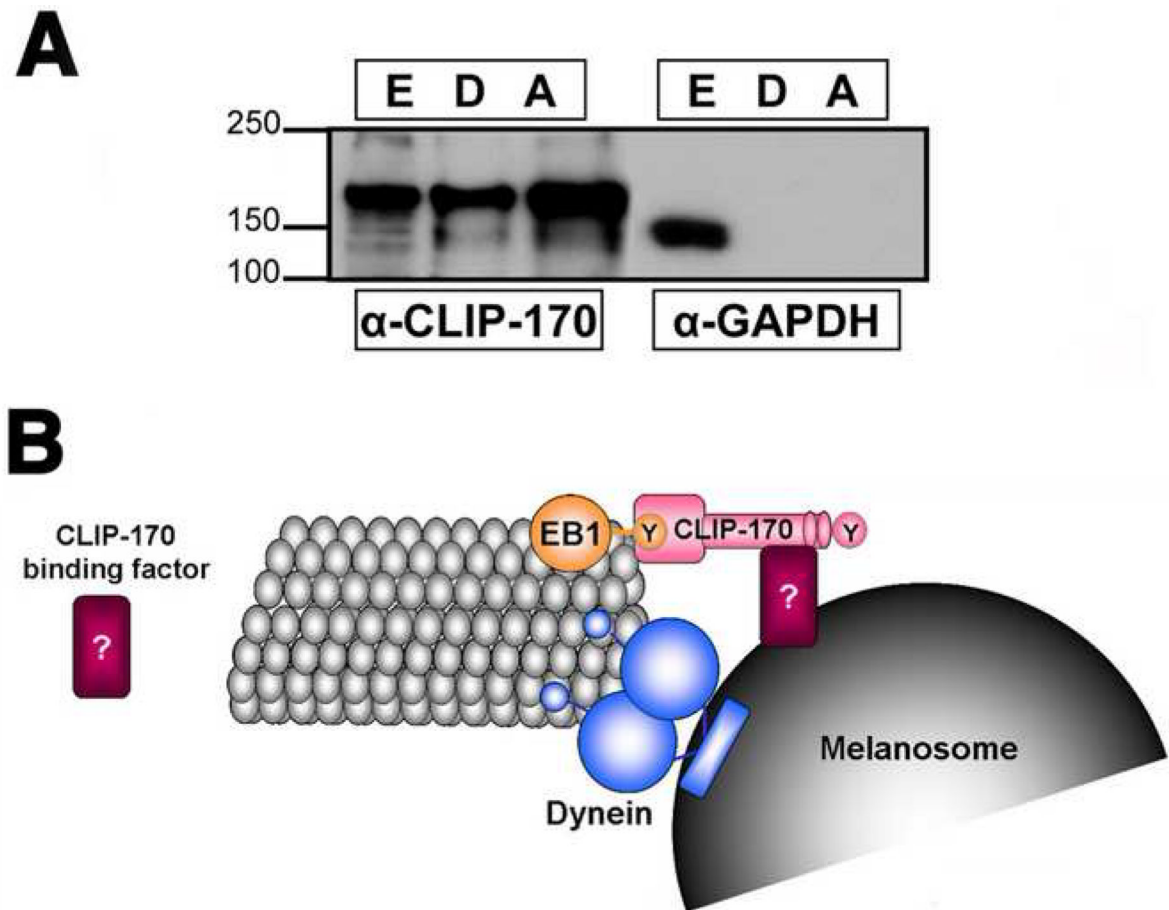
Figure 5. Binding of CLIP-170 to melanosomes
(A) Immunoblotting of cell extract (E) or melanosomes isolated from melanophores with dispersed (D) or aggregated (A) pigment with an antibody against mammalian CLIP-170 (α-CLIP-170; left lanes), or a soluble marker glyceraldehyde-3-phosphate dehydrogenase (α-GAPDH; right lanes). CLIP-170, but not GAPDH co-purifies with melanosomes. Loading of the samples were equalized to compare the amounts of CLIP-170 and GAPDH between the melanosome preparations, and between the fractions of cytosol and melanosome extract by equalizing across the samples concentrations of melanosomes estimated by measuring optical density of the melanosome suspension at 350 nm, and by adjusting the volumes of the melanosome supernatant and extract to the volume of the initial melanosome suspension . (B) Model for CLIP-170 involvement in the binding of melanosomes to MTs. CLIP-170 concentrated at the MT plus end binds an adaptor protein on the melanosome surface, and this binding facilitates the interaction of the pigment granule-bound dynein with the MT lattice.

Table 1

Parameters of MT dynamic instability in melanophores treated with taxol, or overexpressing dominant-negative +TIP constructs

	Taxol	GFP	EB3-GFP	GFP-CLIP-170 head	GFP-CLIP-170 tail	GFP-Lis1
Growth distance (μm)	0.23±0.01 ***	2.96±0.16	3.56±0.20 *	6.81±0.26 ***	6.90±0.45 ***	2.38±0.11 **
Growth rate (μm/s)	0.06±0.01 **	0.17±0.03	0.17±0.03 ~	0.29±0.06 ~	0.22±0.05 ~	0.15±0.05 ~
Shortening distance (μm)	0.23±0.01 ***	3.17±0.18	3.32±0.21 ~	7.13±0.28 ***	9.14±0.64 ***	2.55±0.13 **
Shortening rate (μm/s)	0.06±0.001 **	0.18±0.04	0.19±0.04 ~	0.34±0.06 *	0.27±0.06 ~	0.18±0.01
Catastrophe frequency (s⁻¹)	0.026±0.002 ~	0.026±0.001	0.024±0.001 ~	0.020±0.001 ***	0.013±0.001 ***	0.031±0.001 ***
Rescue frequency (s⁻¹)	0.042±0.002 ***	0.029±0.001	0.026±0.001 *	0.022±0.001 ***	0.017±0.001 ***	0.034±0.001 ***
Duration of pauses (s)	11.51±0.57 ***	3.99±0.31	4.19±0.44 ~	4.13±0.25 ~	3.29±0.15 *	4.38±0.31
Number of analyzed MTs	30	30	40	35	40	40
Number of analyzed cells	6	5	8	6	7	6

Numbers indicate average ± SEM. P values indicate significance of the difference from GFP control.

*
P<0.05

**
P<0.01

***
P<0.001

~
P>0.05

Table 2

Parameters of bidirectional movement of single melanosomes along MTs during pigment aggregation in melanophores overexpressing GFP or dominant-negative +TIP constructs

	GFP	EB3-GFP	GFP-CLIP-170 head	GFP-CLIP-170 tail	GFP-Lis1
Velocity of plus-end runs (nm/s)	345.03±23.63	342.08±17.40***	326.94±20.50***	322.85±15.57***	354.15±21.22***
Length of plus-end runs (nm)	107.68±10.71	91.73±4.85***	83.17±5.40*	87.30±6.23***	95.15±8.06***
Number of examined plus-end runs	309	443	330	405	402
Velocity of minus-end runs (nm/s)	343.75±13.32	381.70±12.81*	343.38±12.07***	350.97±14.51***	375.67±14.98***
Length of minus-end runs (nm)	311.61±25.79	347.09±22.40≈≈	350.12±28.22≈≈	184.66±14.34***	299.85±24.47≈≈
Number of examined minus-end runs	447	589	451	494	536
Duration of pauses (s)	1.03±0.06	0.89±0.04*	0.93±0.06***	1.00±0.06***	0.94±0.06***
Number of examined pauses	211	212	182	181	186
Number of examined trajectories	55	69	57	47	59

Numbers indicate average ± SEM. P values indicate significance of the difference from GFP control.

*
P<0.05

**
P<0.01

***
P<0.001

≈
P>0.05.